

Letter

Optimization of PDE3A Modulators for SLFN12-Dependent Cancer Cell Killing

Timothy A Lewis, Luc de Waal, Xiaoyun Wu, Willmen Youngsaye, Antje Wengner, Charlotte Kopitz, Martin Lange, Stefan Gradl, Manuel Ellermann, Philip Lienau, Stuart L. Schreiber, Heidi Greulich, and Matthew Meyerson

ACS Med. Chem. Lett., **Just Accepted Manuscript** • DOI: 10.1021/acsmchemlett.9b00360 • Publication Date (Web): 18 Oct 2019

Downloaded from pubs.acs.org on October 20, 2019

Just Accepted

“Just Accepted” manuscripts have been peer-reviewed and accepted for publication. They are posted online prior to technical editing, formatting for publication and author proofing. The American Chemical Society provides “Just Accepted” as a service to the research community to expedite the dissemination of scientific material as soon as possible after acceptance. “Just Accepted” manuscripts appear in full in PDF format accompanied by an HTML abstract. “Just Accepted” manuscripts have been fully peer reviewed, but should not be considered the official version of record. They are citable by the Digital Object Identifier (DOI®). “Just Accepted” is an optional service offered to authors. Therefore, the “Just Accepted” Web site may not include all articles that will be published in the journal. After a manuscript is technically edited and formatted, it will be removed from the “Just Accepted” Web site and published as an ASAP article. Note that technical editing may introduce minor changes to the manuscript text and/or graphics which could affect content, and all legal disclaimers and ethical guidelines that apply to the journal pertain. ACS cannot be held responsible for errors or consequences arising from the use of information contained in these “Just Accepted” manuscripts.

Optimization of PDE3A Modulators for SLFN12-Dependent Cancer Cell Killing

Timothy A. Lewis,^{*,†} Luc de Waal,^{†,‡} Xiaoyun Wu,^{†,‡} Willmen Youngsaye,[†] Antje Wengner,[§] Charlotte Kopitz,[§] Martin Lange,[§] Stefan Gradl,[§] Manuel Ellermann,[§] Philip Lienau,[§] Stuart L. Schreiber,[†] Heidi Greulich,^{†,‡} Matthew Meyerson^{†,‡}

[†]Broad Institute of MIT and Harvard, Cambridge, Massachusetts 02142, United States. [‡]Dana-Farber Cancer Institute, Boston, Massachusetts, 01255, United States. [§]Bayer AG, Berlin, Germany.

ABSTRACT: 6-(4-(Diethylamino)-3-nitrophenyl)-5-methyl-4,5-dihydropyridazin-3(2H)-one, or **DNMDP**, potently and selectively inhibits phosphodiesterases 3A and 3B (PDE3A and PDE3B) and kills cancer cells by inducing PDE3A/B interactions with SFLN12. The structure-activity relationship (SAR) of **DNMDP** analogs was evaluated using a phenotypic viability assay, resulting in several compounds with suitable pharmacokinetic properties for *in vivo* analysis. One of these compounds, **BRD9500**, was active in an SK-MEL-3 xenograft model of cancer.

KEYWORDS: PDE3A, SLFN12, DNMDP, HeLa, SK-MEL-3

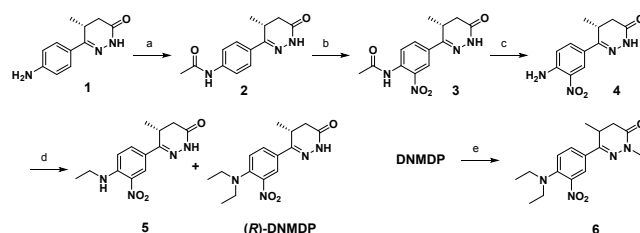
We previously reported on the results of a differential viability screen, where a p53 mutant lung cancer cell line, NCI-H1734, was killed by 6-(4-(diethylamino)-3-nitrophenyl)-5-methyl-4,5-dihydropyridazin-3(2H)-one, or **DNMDP**, while a second lung cancer cell line, A549, was not affected.¹ Further screening detected selective cell killing in 22 out of 766 cancer cell lines, correlating with elevated expression of phosphodiesterase 3A (PDE3A). While **DNMDP** selectively inhibited PDE3, most PDE3 inhibitors had no cell killing effects and in fact rescued cancer cells from **DNMDP**-induced death. PDE3A immunoprecipitation experiments from HeLa cell lysates showed PDE3A bound to Schlafen family member 12² (SFLN12) in the presence of **DNMDP**, but not in the presence of trequinsin, a PDE3 inhibitor that does not kill cancer cells. **DNMDP**-sensitive cell lines were found to express elevated levels of both PDE3A and SFLN12.¹ Since our report, others have discovered that selected PDE3 inhibitors, some of which are known to phenocopy **DNMDP**, kill a gastrointestinal stromal tumor (GIST) cell line³ and a subset of primary ovarian cancer cells.⁴

Although **DNMDP** is a very potent and highly selective compound in a cellular cytotoxicity assay, it has structural liabilities making it unsuitable for further development: a diakylanilino group prone to metabolic instability, and a potentially reactive nitro group. We sought to discover analogs which maintained or improved cellular activity while improving pharmacokinetic properties. Furthermore, we needed potent and selective compounds to better examine the relationship between PDE3 and SFLN12, a protein of unknown function, in sensitive cancer cells. Without sufficient quantities of SFLN12 to study in detail, our initial SAR was driven using phenotypic screening, *i.e.*, viability assays.

The more active (*R*)-enantiomer of **DNMDP** had previously been synthesized¹ from (*R*)-6-(4-aminophenyl)-5-methyl-4,5-dihydropyridazin-3(2H)-one (**1**), a commercially

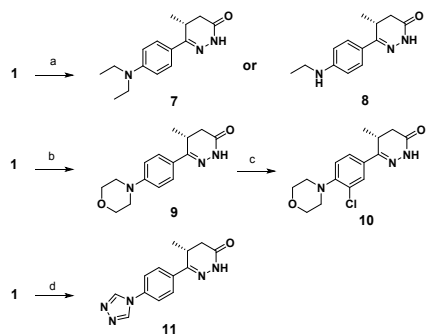
available starting material used for the synthesis of the inotropic drug levosimendan.⁵ Compound **1** was acetylated, then nitrated followed by acetyl hydrolysis. Reductive amination with acetaldehyde produced both the mono and dialkylated amine, (*R*)-**DNMDP**, as a 19:1 ratio of enantiomers as determined by chiral SFC analysis. **DNMDP** was *N*-alkylated producing racemic compound **6**.

Scheme 1. Synthesis of (*R*)-**DNMDP** and Analogs^a



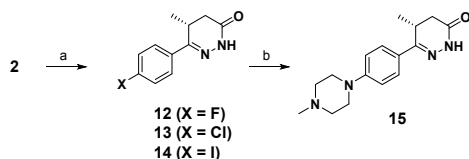
^aReagents and conditions: a) Ac₂O (91%); b) 90% HNO₃/H₂SO₄ (19%); c) NaOH/H₂O/MeOH (quant.); d) CH₃CHO, NaBH(OAc)₃/DCM (7% combined); e) NaH, EtI/DMF (61%).

We were concerned initially that the nitro group of **DNMDP** might lead to promiscuous protein binding. Reductive amination of **1** with acetaldehyde under standard conditions gave *des*-nitro (*R*)-**DNMDP** (**7**) (Scheme 2). The reaction was performed using racemic **1** as well. Modifying reaction conditions allowed isolation of monoethyl analog **8**. Compound **1** was alkylated to make the morpholino analog **9** which was chlorinated adjacent to the morpholine ring (**10**). Heterocycle **11** was prepared by condensation of **1** with diformyl hydrazine.

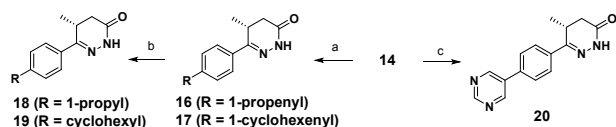
Scheme 2. Synthesis of (*R*)-*des*-Nitro DNMDP Analogs^a

^aReagents and conditions: a) **7** - CH₃CHO, NaBH₃CN/MeOH (82%); **8** - CH₃CHO, then NaBH₃CN/MeOH (8%); b) (BrCH₂CH₂)₂O, K₂CO₃/DMF (46%); c) NaOCl/HOAc (40%); d) CHONHNHCHO (73%).

Diazotization of **1** followed by halogenation produced the fluoro (**12**), chloro (**13**) and iodo (**14**) derivatives, respectively (Scheme 3). Compound **13** (racemic) is a known PDE3 inhibitor.⁶ The iodide **14** reacted at high temperature with *N*-methyl piperazine to produce **15**. Suzuki coupling with **14** followed by hydrogenation gave analogs with cyclic, acyclic, sp² and sp³ carbon substituents on the *para* position of the phenyl ring (**16-19**). Heterocycle **20** was prepared similarly.

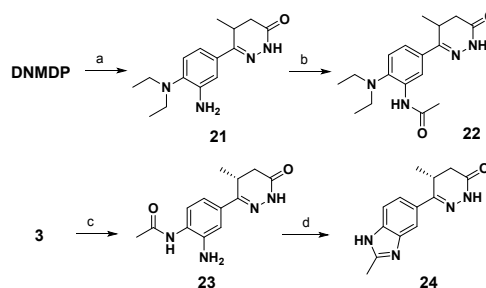
Scheme 3. Synthesis of (*R*)-DNMDP Analogs^a

^aReagents and conditions: a) NaNO₂, HCl/water, then NaBF₄ (**12**, 15%) or CuCl₂ (**13**, 77%) or KI (**14**, 49%); b) *N*-methyl piperazine, NMP, 160 °C microwave (20%).



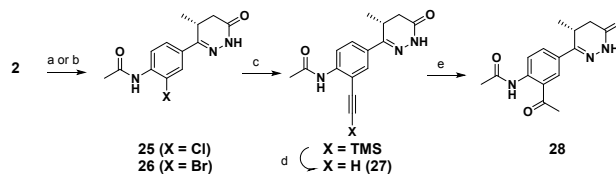
^aReagents and conditions: a) Pd(PPh₃)₄, Na₂CO₃/H₂O/THF, propene (**16**, 90%) or cyclohexene (**17**, 90%); b) H₂, 10% Pd/C, MeOH (60% **18**, 63% **19**); c) 5-pyrimidine boronic acid, Pd(PPh₃)₄, Na₂CO₃/H₂O/dioxane (68%)

Substituent effects on the phenyl ring were examined. The nitro group of DNMDP was reduced and the amine product (**21**) was acetylated (**22**) (Scheme 4). Reducing the nitro group of **3** gave **23**, subsequent heating produced benzimidazole **24**.⁷

Scheme 4. Synthesis of 3-Amino Substituted Analogs^a

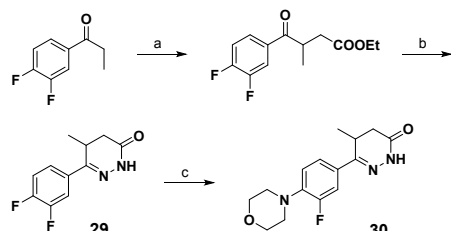
^aReagents and conditions: a) H₂, 10% Pd/C/MeOH (65%); b) Ac₂O (90%); c) H₂, 10% Pd/C/MeOH (92%); d) toluene, reflux (54%).

Halogenation of acetamide **2** provided the chloride (**25**) and bromide (**26**), respectively (Scheme 5). The bromide underwent Sonogishira coupling with trimethylsilylacetylene generating the protected alkyne which was deprotected with fluoride ion to give **27** or hydrolyzed directly to ketone **28**.

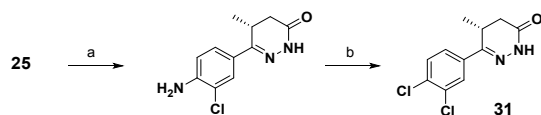
Scheme 5. Synthesis of Acetylene and Acetyl Analogs^a

^aReagents and conditions: a) Br₂, CH₂Cl₂ (15%); b) NaOCl/HOAc (41%); c) **28**, TMSCH, Pd₂(dba)₃, Et₃N/DMF (80%); d) TBAF/THF (52%); e) HCOOH/H₂O (83%).

Fluorinated analogs were prepared starting with 3,4-difluoropropiophenone which was first alkylated with ethyl bromoacetate then condensed with hydrazine to give **29** (Scheme 6). The 4-fluoro group was displaced by refluxing morpholine to give **30**. Racemic **29** and **30** were separated into enantiomers with chiral SCF chromatography. Only one enantiomer of both **29** and **30** was active against HeLa cells, and the active enantiomer of **29** was converted to the active enantiomer of **30**. The absolute stereochemistry of the separated enantiomers was determined by low yielding reductive removal of the fluorine atom from **30** to give **9**. The compound **9** obtained was compared to racemic and (*R*)-**9** by chiral SCF chromatography to assign stereochemistry at the chiral center. The dichloro analog of **29** was enantioselectively synthesized via amide **25**. The amine resulting from hydrolysis was diazotized and converted to dichloro analog **31** (Scheme 6).

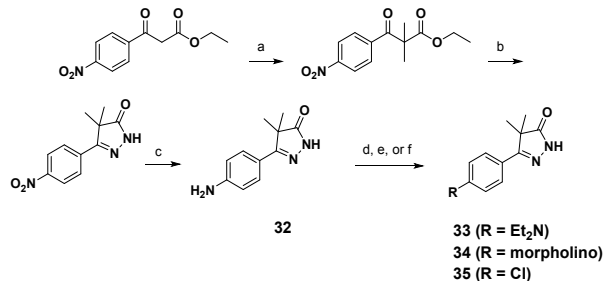
Scheme 6. Synthesis of Dihalogenated Analogs^a

^aReagents and conditions: a) LiHMDS, THF, -78 °C, then BrCH₂COOEt (30%); b) hydrazine/EtOH (29%); c) morpholine, 130 °C (53%).



^aReagents and conditions: a) NaOH/MeOH (98%); b) NaNO₂/HCl then CuCl₂ dihydrate/CH₃CN, 80 °C (58%).

Isosteric replacement of chiral 6-methyl dihydropyridazinones by achiral 5,5-dimethylpyrazolones has maintained PDE3/4 activities in other systems.⁹ Synthesis of this heterocycle began with ethyl 4-nitrobenzoyl acetate which was dimethylated, condensed with hydrazine, and reduced to produce aniline **32** (Scheme 8). Conversion of the amino group of **32** to the diethylamino (**33**), morpholino (**34**) and chloro (**35**) groups was done similarly to the corresponding dihydropyridazinones.

Scheme 7. Synthesis of Dimethylpyrazolones^a

^aReagents and conditions: a) NaH, MeI/THF (40%); b) hydrazine/EtOH (64%); c) H₂, Pd/C/EtOH (94%); d) CH₃CHO, NaBH₃CN/MeOH (56%); e) (BrCH₂CH₂)₂O, K₂CO₃/DMF (33%); f) NaNO₂, HCl/water, then CuCl₂ dihydrate/CH₃CN, 80 °C (72%).

Cellular SAR analysis was performed by treating DNMDP-sensitive HeLa cells with compounds for 3 days at a dose range of 1 nM through 10 μM, with a counterscreen using DNMDP-insensitive A549 cells (Tables 1-2). No compounds tested against A549 cells displayed activity at concentrations up to 10 μM (data not shown)

Table 1. HeLa Cell Viability of DNMDP Analogs^a

Compound	EC ₅₀ (nM)	Compound	EC ₅₀ (nM)
DNMDP	6.9	18	16
(<i>R</i>)-DNMDP	3.8	19	7.7
1	>1000	20	13
5	1.1	21	240
6	>1000	22	>1000
(±)- 7	8.8	23	>1000
(<i>R</i>)- 7	3.3	24	>1000
8	71	(±)- 29	64
(±)- 9	36	(<i>R</i>)- 29	22
(<i>R</i>)- 9	13	(<i>S</i>)- 29	>1000
10	4.5	(±)- 30	2.8
11	>1000	(<i>R</i>)- 30	1.6
12	410	(<i>S</i>)- 30	>1000
13	33	31	4.5
14	7.1	32	>1000
15	310	33	>1000
16	8.8	34	>1000
17	2.2	35	>1000

^a n ≥ 3, std. error ≤ 20%

Several active compounds, (*R*)-**7**, (*R*)-**30**, and **31**, were tested in HeLa cells at effective doses and treated with varying levels of trequinsin (PDE IC₅₀ 0.25 nM¹⁰). As was seen previously with DNMDP,¹ dose dependent cell rescue was observed indicating a similar mechanism of action.

We previously reported that the (*R*)-enantiomer of DNMDP is 200-500 times more active, depending upon the cell line tested, than the (*S*)-enantiomer.¹ This stereochemical dependence was seen in four new examples, where the (*R*)-enantiomer was more active than the (*S*)-enantiomer or the racemate (**7**, **9**, **29**, **30**).

Removing one ethyl group from DNMDP (**5**) had little effect on potency, while *N*-ethylating the dihydropyridazinone ring (**6**) diminished activity. Removing the nitro group from DNMDP did not have a deleterious effect (**7**). Reduction of the nitro group of DNMDP (**21**) reduced activity and acylation of the resulting amine (**22**) removed activity.

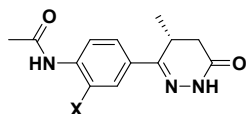
The diethylamino group of (*R*)-*des*-nitro DNMDP (**7**) could be replaced by a morpholine ring (**9**). The *N*-methylpiperazine analog (**15**) displayed much less activity. The presence of a fluorine atom adjacent to the morpholine nitrogen (**30**), as found in the antibiotic linezolid,¹¹ improved activity in the racemic and (*R*)-examples, while the (*S*)-enantiomer was still inactive. Substitution of fluorine with chlorine maintained activity (**10**). Replacement of the diethylamino group with heterocycles on (*R*)-*des*-nitro DNMDP (**7**) lead to both active (**20**) and inactive (**24**, **11**) compounds.

Replacing the diethylamino group of *des*-nitro DNMDP (**7**) with halogens chloro (**13**) and iodo (**14**) was permitted, while the fluoro analog was significantly less active (**12**). As was the case with a 4-morpholino group, adding an additional halogen at the 3-position improved activity (**29/12**, **31/13**). Substitution with carbon substituents (**16-19**) retained cellular activity.

The dimethyl pyrrolidinones (**32-35**) were inactive.

Intermediate acetamides were tested (Table 2). Contrary to the case with the diethylamino analogs (**7** and **DNMDP**), the *des*-nitro analog **2** had no activity whereas the nitrated analog **3** was very potent. Electron withdrawing substituents improved activity, but an amino group was not tolerated (**25**).

Table 2. HeLa Cell Viability of Acylated Amines^a



Compound	X	EC ₅₀ (nM)
2	H	>1000
3	NO ₂	4.9
23	NH ₂	>1000
25	Cl	24
26	Br	21
27	CCH	65
28	Ac	130

^a n ≥ 3, std. error ≤ 20%

We extended our cellular testing beyond HeLa cells to the **DNMDP**-sensitive NCI-H2122 (lung cancer) and COLO741 (melanoma) cell lines, as well as the **DNMDP**-insensitive HCT116 (colorectal cancer) and IMR90 (normal lung fibroblast) cell lines. The results mirror those using HeLa and A549 cells; active compounds are only slightly less active against H2122 and COLO741 cell lines, and all the compounds are inactive against the HCT116 and IMR-90 cells (Supporting Information Table 1).

While the mechanism of action of our compounds involves inducing PDE3/SLFN12 interaction, we nonetheless tested some of our compounds for biochemical inhibition of PDE3A and PDE3B (Table 3).¹² No major selectivity for one isozyme over the other was observed, and the HeLa activity generally mirrored the biochemical results. Halogenation of the phenyl ring (**9** to **(R)**-**30**) increased PDE3A/B biochemical inhibition ten-fold. The cellular SAR generally agreed with reported SAR of PDE3 inhibition¹³ with the *(R)*-enantiomers being more potent.¹⁴ However, as was seen previously with commercially available PDE3 inhibitors, some **DNMDP** analogs, *e.g.* **2**, were potent PDE3 inhibitors with no cellular activity. The increase in cellular potency relative to biochemical activity for active compounds (HeLa EC₅₀s 2.4-15 fold lower than PDE3A/B average IC₅₀s) is consistent with neomorphic modulation, due to complex formation with SLFN12 in this case (see below).

Table 3. PDE3 Inhibition and HeLa Viability^a

Compound	IC ₅₀ (nM)		EC ₅₀ , HeLa (nM)
	PDE3A	PDE3B	
DNMDP	25	100	6.9
9	120	260	13
(R) - 30	10	27	1.6
31	8	14	4.5
15	2000	3500	310
2	24	16	>1000
25	8	10	24

^aIC₅₀s are an average of two values

Attempts to find other molecular targets of our compounds were unsuccessful. A Millipore Kinase Profiler screen of **DNMDP** found no inhibition (conc. 10 μM) against 234 kinases.¹ A Eurofins Lead Profiling screen of compound **9** (conc. 10 μM, 68 assays) found no interactions with a non-kinase targets (Supporting Information Table 2).

Previously we used mass spectrometry proteomic analysis to demonstrate that **DNMDP** binds to PDE3A, inducing PDE3A binding to SLFN12, which results in cell killing whereas non-toxic PDE3 inhibitors do not induce PDE3A/SLFN12 complex formation.¹ To observe compound-induced PDE3/SLFN12 interaction with newer compounds we transfected HeLa cells with a plasmid that expresses SLFN12 fused with a V5 epitope tag. We then treated the cells with **DNMDP** or **(R)**-**30** (10 μM). After 8 hours of compound treatment the cells were lysed and endogenous PDE3A protein was immunoprecipitated using an anti-PDE3A antibody. SLFN12 co-immunoprecipitation was analyzed by immunoblotting with an anti-V5 antibody to detect the SLFN12-V5 fusion protein. The SLFN12-V5 was clearly detected with the anti-V5 antibody for both **DNMDP** and **(R)**-**30**, indicating that both compounds stabilize the PDE3A-SLFN12 interaction (Figure 1).

Cell death with **DNMDP** occurs via apoptosis by an as of yet determined mechanism.¹ A recent article reports PDE3A/SLFN12 interaction being induced by high concentration of 17-β-estradiol, leading to HeLa cell death which can be rescued by the PDE3 inhibitors cilostazole and trequinsin, as seen with **DNMDP**-induced HeLa cell death.¹⁵ The stabilization of SFLN12 leads to a decrease in translation of anti-apoptotic proteins leading to cell death.¹⁵

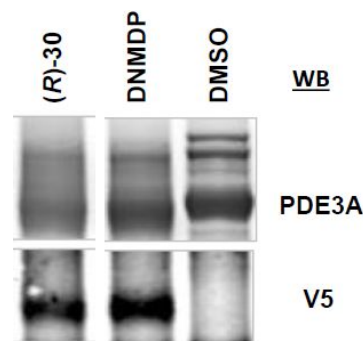


Figure 1. Detection of PDE3A/SLFN12 Binding

The *in vitro* pharmacokinetic properties of selected active compounds were determined (Table 4). Overall the properties were good, and all compounds were highly soluble (>70 μM). Removal of the nitro group from **DNMDP** (**7**) and replacing the diethylamino group with a morpholine (**9**) improved microsomal stability. Addition of a fluorine atom (**30**) was well tolerated. Halogenated analogs (**13**) were stable to microsomes as was one heterocyclic analog (**20**). Other carbon substituted analogs (**16**, **18**) were unstable to microsomes. Plasma protein binding of the analogs generally correlated with cLogP, with the more polar compounds

displaying less protein binding. Plasma stability, mouse and human, was >80% at 5 hours for all compounds tested.

Table 4. Pharmacokinetic In Vitro Properties of Select Compounds^a

Compound	Microsomal stability (% remaining at 1 h)		Plasma Protein Binding (% bound)		Plasma Stability (% remaining at 5 h)	
	h	m	h	m	h	m
DNMDP	95	23	87	92	85	87
7	89	26	90	90	104	96
9	94	99	47	42	87	105
(±)-30	109	102	57	55	80	101
(±)-29	108	82	56	52	93	96
13	81	92	87	81	93	86
20	83	105	56	54	104	108

^ah = human, m = mouse, values are average of three values

Compound (*R*)-30, a.k.a. **BRD9500**, was profiled to determine its suitability for animal studies. Compound (*R*)-30 does not inhibit other phosphodiesterases tested (Supporting Information Table 3). No inhibition in a cytochrome P450 panel (CYPs 1A2, 2C8, 2C9, 2D6, and 3A4) was detected when tested at high concentrations. Compound (*R*)-30 is soluble (ca. 1 mM), permeable (Caco2 A-B 279 nm/s; B-A 198 nm/s, efflux ratio 0.71) and stable in solution at various pH levels (1, 7, and 10) for extended time periods. An Ames test was negative and no hERG interaction was detected at high concentration. (*R*)-30 showed high plasma levels in mice after iv (1 mg/kg) as well as po (2 mg/kg) dosing over eight hours making it a valuable candidate for *in vivo* xenograft testing (Supporting Information Table 4).

HeLa proved to be a convenient and robust cell line for viability assays, but for xenograft experiments we chose to work with a cancer cell line more relevant to therapeutic opportunities. Viability assays were performed under identical procedures using the SK-MEL-3 melanoma cell line with eight compounds (Table 5). Gratifyingly, the SK-MEL-3 EC₅₀ values were similar to those of HeLa.

Table 5. Viability with SK-MEL-3 Cells

Compound	EC ₅₀ (nM)	Compound	EC ₅₀ (nM)
DNMDP	12	15	684
13	29	9	11
(<i>R</i>)-30	1.3	31	5.6
3	4.2	25	31

^an = 3, std. error < 10%

The anti-tumor activity of compound (*R*)-30 was evaluated in tumor xenografts derived from SK-MEL-3 melanoma cells that were subcutaneously inoculated into female NMRI nude mice (Figure 2). (*R*)-30 was applied orally at 10 and 20 mg/kg twice daily (2QD) and at 50 mg/kg once per day (QD). We observed inhibition of tumor growth upon all (*R*)-30 treatments, achieving strongest anti-tumor activity at 50 mg/kg QD with a T/C_{rel.area} of 0.09 and T/C_{weight} of 0.16 (p < 0.001 and p < 0.05 vs vehicle, respectively). All treatments were

well tolerated without critical body weight loss (>10%) or toxicities (Supporting Information Figure 1).

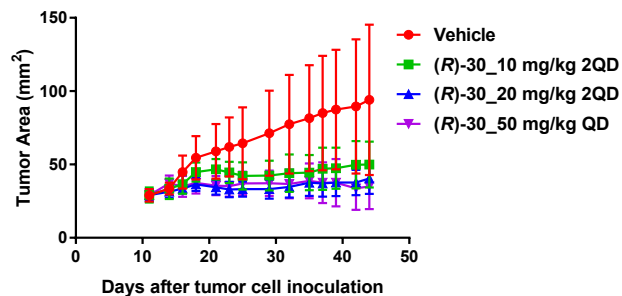


Figure 2. Anti-tumor efficacy of (*R*)-30 in the SK-MEL-3 tumor model in NMRI nude mice

Plasma levels of (*R*)-30 were monitored throughout the xenograft experiment (Figure 3). With a dose of 50 mg/kg QD the unbound plasma level of (*R*)-30 at 24 h was >100-fold the EC₅₀ against SK-MEL-3 cells, and at doses of 10 and 20 mg/kg 2QD the EC₅₀ was covered for >30-fold at 24 h (Figure 3).

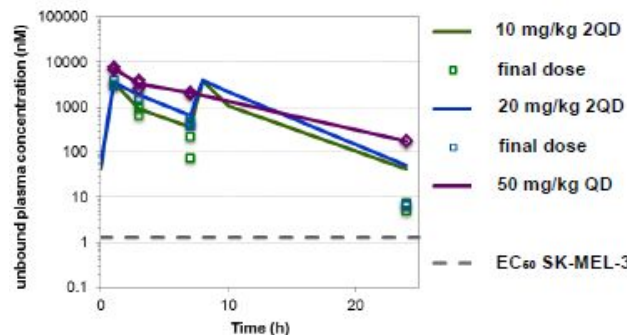


Figure 3. Unbound plasma levels of (*R*)-30 on day 45 after final dose to SK-MEL-3 bearing NMRI nude mice. Curves for lower dose 2QD simulated.

In summary, starting with our initial screening hit **DNMDP**, compounds were optimized using a cellular viability assay, making them not only more potent, but improving upon their pharmacological properties. The increase in cellular potency correlated with an increase in PDE3 inhibition, though most known PDE3 inhibitors do not kill HeLa cells. Our advanced compound, (*R*)-30/**BRD9500**, induced PDE3A/SLFN12 binding in HeLa cells and was active with oral dosing in a mouse xenograft model of melanoma. Current studies are focused on determining the mechanism of action of small molecule modulators of PDE3 and SLFN12 leading to cancer cell death.

ASSOCIATED CONTENT

Supporting Information

The Supporting Information is available free of charge on the ACS Publications website at

Synthesis and characterization of all compounds, biological assay procedures, and *in vivo* experiment details (PDF)

AUTHOR INFORMATION

Corresponding Author

*E-mail: tlewis@broadinstitute.org

ORCID

Timothy A. Lewis: 0000-0001-9748-9575

Stuart L. Schreiber: 0000-0003-1922-7558

Author Contributions

T.A.L., W.Y., and S.G. designed and synthesized compounds, L.d.W., X.W., and M.L. tested compounds, P.L. supervised pharmacokinetic studies, A.W. and C.K. performed the in vivo study, T.A.L., S.L.S., H.G., and M.M. directed the project and wrote the manuscript which has been approved by all the authors.

Funding Sources

The authors would like to thank the US National Institutes of Health's Molecular Libraries Program Centers Network (MLPCN) (grant number 3U45HG005032-05S1 to S.L.S.)¹⁶ and Bayer for financial support.

ACKNOWLEDGMENTS

We are grateful to Steven Johnson (Broad Institute) for in vitro pharmacokinetic data.

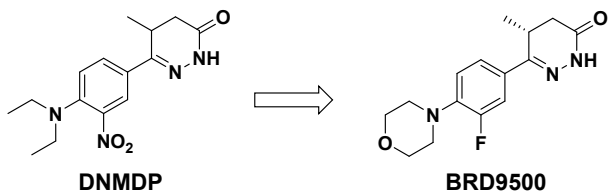
ABBREVIATIONS

PDE3, phosphodiesterase 3; SLFN12, Schlafen family member 12; DNMDP, 6-(4-(diethylamino)-3-nitrophenyl)-5-methyl-4,5-dihydropyridazin-3(2H)-one; NMP, N-methyl-2-pyrrolidinone; TMSCCH, trimethylsilylacetylene; dba, dibenzylideneacetone; TBAF, tetrabutylammonium fluoride; LiHMDS, lithium hexamethyldisilazane

REFERENCES

- 1) de Waal, L.; Lewis, T.A.; Rees, M.G.; Tsherniak, A.; Wu, X.; Choi, P.S.; Gechijian, L.; Hartigan, C.; Faloon, P.W.; Hickey, M.J.; Tolliday, N.; Carr, S.A.; Clemons, P.A.; Munoz, B.; Wagner, B.K.; Shamji, A.F.; Koehler, A.N.; Schenone, M.; Burgin, A.B.; Schreiber, S.L.; Greulich, H.; Meyerson, M. Identification of cancer-cytotoxic modulators of PDE3A by predictive chemogenomics. *Nat. Chem. Biol.* **2016**, *12*, 102-8.
- 2) Puck, A.; Aigner, R.; Modak, M.; Cejka, P.; Blaas, D.; Stöckl, J. Expression and regulation of Schlafen (SLFN) family members in primary human monocytes, monocyte-derived dendritic cells and T cells. *Results Immunol.* **2015**, *5*, 23-32.
- 3) Vandenberghe, P.; Hagué, P.; Hockman, S.C.; Manganiello, V.C.; Demetter, P.; Erneux, C.; Vanderwinden, J.M. Phosphodiesterase 3A: a new player in development of interstitial cells of Cajal and a prospective target in gastrointestinal stromal tumors (GIST). *Oncotarget* **2017**, *8*, 41026-41043.
- 4) Nazir, M.; Senkowski, W.; Nyberg, F.; Blom, K.; Edqvist, P.H.; Jarvius, M.; Andersson, C.; Gustafsson, M.G.; Nygren, P.; Larsson R.; Fryknäs, M. Targeting tumor cells based on Phosphodiesterase 3A expression. *Exp. Cell Res.* **2017**, *361*, 308-315.
- 5) Szilágyi, S.; Pollesello, P.; Levijoki, J.; Kaheinen, P.; Haikala, H.; Edes, I.; Papp, Z. The effects of levosimendan and OR-1896 on isolated hearts, myocyte-sized preparations and phosphodiesterase enzymes of the guinea pig. *Eur. J. Pharmacol.* **2004**, *486*, 67-74.
- 6) Robertson, I. M.; Baryshnikova, O. K.; Li, M. X.; Sykes, B. D. Defining the binding site of levosimendan and its analogues in a

- regulatory cardiac troponin C-troponin I complex. *Biochemistry* **2008**, *47*, 7485-7495.
- 7) Zhao, H.; Fu, H.; Qiao, R. Copper-catalyzed direct amination of ortho-functionalized haloarenes with sodium azide as the amino source. *J. Org. Chem.* **2010**, *75*, 3311-3316.
- 8) Ochiai, K.; Takita, S.; Kojima, A.; Eiraku, T.; Ando, N.; Iwase, K.; Kishi, T.; Ohinata, A.; Yageta, Y.; Yasue, T.; Adams, D.R.; Kohno, Y. 4,4-Dimethylpyrazolone replacement: Phosphodiesterase inhibitors. Part 4: design, synthesis and structure-activity relationships of dual PDE3/4-inhibitory fused bicyclic heteroaromatic-4,4-dimethylpyrazolones. *Bioorg. Med. Chem Lett.* **2012**, *22*, 5833-8.
- 9) Cignarella, G.; Barlocco, D.; Pinna, G.A.; Loriga, M.; Curzu, M. M.; Tofanetti, O.; Germini, M.; Cazzulani, P.; Cavalletti, E. Synthesis and biological evaluation of substituted benzo[h]-cinnolinones and 3H-benzo[6,7]cyclohepta[1,2-c]pyridazinones: higher homologs of the antihypertensive and antithrombotic 5H-indeno[1,2-c]pyridazinones. *J. Med. Chem.* **1989**, *32*, 2277-2282.
- 10) Ruppert, D.; Weithmann, K. U. HL 725, an extremely potent inhibitor of platelet phosphodiesterase and induced platelet aggregation in vitro. *Life Sci.* **1982**, *31*, 2037-43.
- 11) Barbachyn, M. R.; Ford, C. W. Oxazolidinone structure-activity relationships leading to linezolid. *Angew. Chem. Int. Ed. Eng.* **2003**, *42*, 2010-2023.
- 12) In vitro PDE3 assays were performed at BPS Bioscience, San Diego, CA, www.bpsbioscience.com.
- 13) Moos, W.H.; Humblet, C.C.; Sircar, I.; Rithner, C.; Weisharr, R.E.; Bristol, J.A.; McPhail, A.T. Cardiotoxic agents: 8. Selective inhibitors of adenosine 3',5'-cyclic phosphate phosphodiesterase III. Elaboration of a five-point model for positive inotropic activity. *J. Med. Chem.* **1987**, *30*, 1963-1972.
- 14) Owings, F.F.; Fox, M.; Kowalski, C.J.; Baine, N.H. An enantioselective synthesis of SK&F 93505, a key intermediate for preparing cardiotoxic agents. *J. Org. Chem.* **1991**, *56*, 1963-1966.
- 15) Li, D.; Chen, J.; Ai, Y.; Gu, X.; Li, L.; Che, D.; Jiang, Z.; Li, L.; Chen, S.; Huang, H.; Wang, J.; Cai, T.; Cao, Y.; Qi, X.; Wang, X. Estrogen-related hormones induce apoptosis by stabilizing Schlafen-12 protein turnover. *Mol. Cell* **2019**, *75*, 1103-1116.
- 16) Lewis, T.A.; de Waal, L.; Youngsaye, W.; Gechijian, L.; Hickey, M.; Faloon, P.; Mikse, O.; Dandapani, S.; Wong, K.; Tolliday, N.; Munoz, B.; Palmer, M.; Greulich, H.; Meyerson, M.L.; Schreiber, S.L. A candidate cell-selective anticancer agent. Probe Reports from the NIH Molecular Libraries Program [Internet]. Bethesda (MD): National Center for Biotechnology Information (US); 2010-2013 Dec 12 [updated 2014 Sep 18].



10
11
12
13
14

EC₅₀ 12 nM (SK-MEL-3)
racemic
unstable to microsomes

EC₅₀ 1 nM (SK-MEL-3)
enantiomerically pure
active in xenograft

15
16
17
18
19
20
21
22
23
24
25
26
27
28
29
30
31
32
33
34
35
36
37
38
39
40
41
42
43
44
45
46
47
48
49
50
51
52
53
54
55
56
57
58
59
60

Insert Table of Contents artwork here